PHYSICAL REVIEW D **89,** 014022 (2014)

Inclusive semileptonic fits, heavy quark masses, and V_{cb}

Paolo Gambino
Dipartimento di Fisica, Università di Torino, and INFN Torino, I-10125 Torino, Italy

Christoph Schwanda
Institut für Hochenergiephysik, 1050 Wien, Austria
(Received 22 July 2013; published 24 January 2014)

We perform global fits to the moments of semileptonic B-decay distributions and extract $|V_{cb}|$, the heavy quark masses, and the nonperturbative parameters of the heavy quark expansion. We include next-to-next-to-leading-order perturbative corrections and recent determinations of the charm mass and discuss how they improve the precision of the global fit. In particular, using the m_c determination of Chetyrkin *et al.* [Phys. Rev. D**80**, 074010 (2009)], we get $m_b^{\rm kin} = 4.541(23)$ GeV and $|V_{cb}| = (42.42 \pm 0.86) \times 10^{-3}$. We also discuss the implications of the new fits for the normalization of rare B decays, the zero-recoil sum rule in $B \to D^* \ell \nu$, and the inclusive determination of $|V_{ub}|$.

DOI: 10.1103/PhysRevD.89.014022 PACS numbers: 13.25.Hw, 14.40.Nd, 12.15.Hh, 12.15.Ff

I. INTRODUCTION

The Cabibbo-Kobayashi-Maskawa (CKM) matrix elements V_{cb} and V_{ub} are important ingredients in the analyses of CP violation in the Standard Model and in the search for new physics in flavor-violating processes. For instance, the absolute value of their ratio gives one of the sides of the unitarity triangle, and the ε_K constraint on $\bar\rho$ and $\bar\eta$ is very sensitive to the precise value of $|V_{cb}|$; see Ref. [1] for recent analyses. The determination of V_{cb} and V_{ub} from inclusive semileptonic B decays is based on an operator product expansion (OPE) that allows us to express the widths and the first moments of the kinematic distributions of $B \to X_{u,c} \ell \nu$ as double expansions in α_s and $\Lambda_{\rm QCD}/m_b$. The leading terms in these double expansions are given by the free b quark decay, and the first corrections are $O(\alpha_s)$ and $O(\Lambda_{\rm QCD}^2/m_b^2)$ [2].

The relevant parameters of the double expansions are the heavy quark masses m_b and m_c, the strong coupling α_s, and the B-meson matrix elements of local operators of growing dimension: μ_π^2 and μ_G^2 at $O(1/m_b^2)$, ρ_D^3 and $\rho_{\rm LS}^3$ at $O(1/m_b^3)$, etc. The latter can be constrained by various moments of the lepton energy and hadron mass distributions of $B \to X_c \ell \nu$ that have been measured with good accuracy at the B factories, as well as at CLEO, DELPHI, and CDF. The total semileptonic width can then be employed to extract $|V_{cb}|$. The situation is less favorable in the case of $|V_{ub}|$, in which the total rate is much more difficult to access experimentally, but the results of the semileptonic fits are crucial in that case as well; see Ref. [3] for a review. This strategy has been rather successful and has allowed for a $\sim$2% determination of V_{cb} and for a $\sim$5% determination of V_{ub} from inclusive decays [4].

Complementary studies of exclusive decays and nonperturbative calculations of the relevant form factors have also progressed considerably, reaching a similar level of accuracy. Unfortunately, a $\sim 2\sigma$ discrepancy persists between the most precise determinations of $|V_{cb}|$: the inclusive one and the one based on $B \to D^* \ell \nu$ at zero recoil and a lattice calculation of the form factor [4,5]. However, the zero-recoil form-factor estimate based on heavy quark sum rules leads to $|V_{cb}|$ in good agreement with the inclusive result [6]. A stronger discrepancy between the inclusive and exclusive determinations occurs in the case of $|V_{ub}|$ [4].

The importance of a precise and reliable extraction of $|V_{cb}|$ and of the inputs for the inclusive $|V_{ub}|$ analysis has motivated us to critically reexamine the procedure used in the semileptonic fits almost a decade after the first comprehensive studies [7–9]. There are three relevant issues in this respect: (i) the theoretical uncertainties and how they are implemented in the fit, (ii) the inclusion of additional constraints on the parameters, and (iii) the need to update the theoretical predictions to next-to-next-to-leading order (NNLO).

For what concerns the theoretical uncertainties, we have already observed [10] a marked dependence of the results on the ansatz for the correlations among theoretical uncertainties at different values of the cut on the lepton energy. In this paper, we discuss different options and compare the results of the fits performed accordingly.

Regarding the inclusion of additional constraints from other processes, we recall that the semileptonic moments are sensitive to a linear combination of m_c and m_b but cannot resolve the individual masses with good accuracy. To improve the accuracy of the fit, the moments of the photon energy in $B \to X_s \gamma$ have generally been employed, but in the last few years, quite precise determinations of the heavy quark masses by completely different methods (e^+e^- sum rules, lattice QCD, etc.) have become available, see, e.g., Refs. [11–15]. Radiative moments remain very interesting, but they are not competitive with the charm

mass determinations and are, in principle, subject to additional $O(\Lambda_{\rm QCD}/m_b)$ effects, which have not yet been estimated [16]. Here, we will discuss the inclusion of the most recent heavy quark mass determinations in the semileptonic fit. As we will see, these precise external inputs reduce the dependence on the assumptions regarding the theoretical correlations.

Recent progress has made it necessary to update the theoretical predictions used in the fits. The NNLO $O(\alpha_s^2)$ calculation has been completed [17–19] and implemented [20] in a code that has been used in preliminary analyses by the Heavy Flavor Averaging Group [4]. This code extends and improves on the kinetic scheme calculation of Ref. [21], used in Refs. [7,9], and forms the basis of the present work. The NNLO accuracy is a necessary prerequisite for using the precise heavy quark mass constraints we have just mentioned. Concerning the perturbative corrections to the Wilson coefficients of power-suppressed operators, the $O(\alpha_s\mu_\pi^2/m_b^2)$ were computed in Refs. [22,23]. However, the $O(\alpha_s\mu_G^2/m_b^2)$ corrections are not yet available, and here we will not include any $O(\alpha_s/m_b^2)$ corrections. Concerning higher-order power corrections, the $O(1/m_b^4)$ and $O(1/m_Q^5)$ effects have been computed [24]. The main problem here is a proliferation of nonperturbative parameters that cannot all be fitted from experiment. In Ref. [24], they were estimated in the ground-state saturation approximation, leading to a final $O(1/m_Q^{4,5})$ effect on $|V_{cb}|$ of $+0.4\%$. This may well be the order of magnitude of higher-order power corrections, but further investigations are necessary, also because sizable effects beyond the ground state saturation approximation have been found [6]. Here, we include only effects up to $O(1/m_b^3)$ [25].

The paper is organized in the following way. We first discuss the relevant observables and list all the moment measurements included in our fits. Then, in Sec. III, we explain our estimate of theoretical errors and discuss several options for their correlations. In Sec. IV, we consider the inclusion of independent constraints on m_c and m_b in the fits and study their impact on the results; then, in Sec. V, we consider a few relevant applications of the fits. Finally, Sec. VI contains a summary of our results.

II. OBSERVABLES INCLUDED IN THE FITS

The first few moments of the charged lepton energy spectrum in inclusive $b\to c\ell\nu$ decays are experimentally measured with high precision—better than 0.2% in the case of the first moment. At the B factories, a lower cut on the lepton energy, $E_\ell \geq E_{\rm cut}$, is applied to suppress the background. Experiments measure the moments at different values of $E_{\rm cut}$, which provides additional information as the cut dependence is also a function of the OPE parameters. The relevant quantities are therefore

$$\langle E_\ell^n\rangle_{E_\ell>E_{\rm cut}} = \frac{\int_{E_{\rm cut}}^{E_{\rm max}} dE_\ell E_\ell^n \frac{d\Gamma}{dE_\ell}}{\int_{E_{\rm cut}}^{E_{\rm max}} dE_\ell \frac{d\Gamma}{dE_\ell}}, \tag{1}$$

which are measured for n up to 4, as well as the ratio R^* between the rate with and without a cut,

$$R^*(E_{\rm cut}) = \frac{\int_{E_{\rm cut}}^{E_{\rm max}} dE_\ell \frac{d\Gamma}{dE_\ell}}{\int_0^{E_{\rm max}} dE_\ell \frac{d\Gamma}{dE_\ell}}. \tag{2}$$

This quantity is needed to relate the actual measurement of the rate with a cut to the total rate, from which one conventionally extracts $|V_{cb}|$. Since the physical information that can be extracted from the first three linear moments is highly correlated, it is more convenient to study the central moments, namely, the variance and asymmetry of the lepton energy distribution. In the following, we will consider only R^* and

$$\begin{aligned} \ell_1(E_{\rm cut}) &= \langle E_\ell\rangle_{E_\ell>E_{\rm cut}}, \\ \ell_{2,3}(E_{\rm cut}) &= \langle (E_\ell - \langle E_\ell\rangle)^{2,3}\rangle_{E_\ell>E_{\rm cut}}. \end{aligned} \tag{3}$$

Similarly, in the case of the moments of the hadronic invariant mass distribution, we consider

$$\begin{aligned} h_1(E_{\rm cut}) &= \langle M_X^2\rangle_{E_\ell>E_{\rm cut}}, \\ h_{2,3}(E_{\rm cut}) &= \langle (M_X^2 - \langle M_X^2\rangle)^{2,3}\rangle_{E_\ell>E_{\rm cut}}. \end{aligned} \tag{4}$$

These observables can be expressed as double expansions in α_s and inverse powers of m_b, schematically,

$$\begin{aligned} M_i = M_i^{(0)} + \frac{\alpha_s(\mu)}{\pi} M_i^{(1)} + \left(\frac{\alpha_s}{\pi}\right)^2 M_i^{(2)} + M_i^{(\pi)} \frac{\mu_\pi^2}{m_b^2} \\ + M_i^{(G)} \frac{\mu_G^2}{m_b^2} + M_i^{(D)} \frac{\rho_D^3}{m_b^3} + M_i^{(\rm LS)} \frac{\rho_{\rm LS}^3}{m_b^3} + \cdots, \end{aligned} \tag{5}$$

where all the coefficients $M_i^{(j)}$ depend on m_c, m_b, $E_{\rm cut}$, and on various renormalization scales. The OPE parameters μ_π^2, … are matrix elements of local b-field operators evaluated in the physical B meson, i.e., without taking the infinite mass limit. The dots represent missing terms of $O(\alpha_s/m_b^2)$ and $O(1/m_b^4)$, which are either unknown or which we do not include for the reasons explained in the Introduction. We work in the kinetic scheme [26] and follow the implementation described in Refs. [20,21]. In particular, in the hadronic moments, we do not expand in powers of $\bar\Lambda = M_B - m_b$. While we always express the bottom mass and the four relevant expectation values that appear in Eq. (5) in the kinetic scheme, setting the cutoff $\mu^{\rm kin}$ at 1 GeV, we will use both the kinetic and the $\overline{\rm MS}$ schemes for the charm mass and denote it with $m_c^{\rm kin}(\mu^{\rm kin})$ and $\bar m_c(\bar\mu)$, respectively. Unless otherwise specified, we evaluate α_s at $\mu_0 = 4.6$ GeV and assume $\alpha_s(\mu_0) = 0.22$.

A change of ± 0.005 around this value leads to small changes in the results of our fits (about 1 MeV in m_b), always much smaller than their final uncertainty.

The experimental data for the moments are fitted to the theoretical expressions in order to gain information on the nonperturbative parameters and the heavy quark masses, which we then employ to extract $|V_{cb}|$. Table I shows the 43 measurements of the moments that we always include in the fits, unless otherwise specified. The chromomagnetic expectation value μ_G^2 is also constrained by the hyperfine splitting

$$M_{B^*} - M_B = \frac{2}{3}\frac{\mu_G^2}{m_b} + O\left(\frac{\alpha_s \mu_G^2}{m_b}, \frac{1}{m_b^2}\right).$$

Unfortunately, little is known of the power corrections to the above relation, and only a loose bound can be set; see Ref. [6] for a recent discussion. For what concerns $\rho_{\rm LS}^3$, it is somewhat constrained by the heavy quark sum rules. Following Refs. [6,21,27], we will therefore use in our fits the constraints

$$\begin{aligned} \mu_G^2 &= (0.35 \pm 0.07)\ \text{GeV}^2, \\ \rho_{\rm LS}^3 &= (-0.15 \pm 0.10)\ \text{GeV}^3. \end{aligned} \tag{6}$$

It should be stressed that $\rho_{\rm LS}^3$ plays a minor role in the fits because its coefficients are generally suppressed with respect to the other parameters.

We now perform a first global fit, without any theoretical uncertainty. The fit is not good, with $\chi^2/\text{degrees of freedom} \sim 2$, corresponding to a very small p value and driven by a strong tension ($\sim 3.5\sigma$) between the constraints in Eq. (6) and the measured moments. If we drop the constraints of Eq. (6), the fit is not too bad. It is then clear from the outset that theoretical uncertainties are not so necessary for the OPE expressions to fit the moments—which would merely test Eq. (5) as a parametrization; they are instead needed to preserve the definition of the parameters as B expectation values of certain local operators, which in turn can be employed in the semileptonic widths and in other applications of the heavy quark expansion.

TABLE I. Experimental data used in the fits unless otherwise specified.

	Experiment	Values of $E_{\rm cut}$ (GeV)	Ref.
R^*	*BABAR*	0.6, 1.2, 1.5	[28,29]
ℓ_1	*BABAR*	0.6, 0.8, 1, 1.2, 1.5	[28,29]
ℓ_2	*BABAR*	0.6, 1, 1.5	[28,29]
ℓ_3	*BABAR*	0.8, 1.2	[28,29]
h_1	*BABAR*	0.9, 1.1, 1.3, 1.5	[28]
h_2	*BABAR*	0.8, 1, 1.2, 1.4	[28]
h_3	*BABAR*	0.9, 1.3	[28]
R^*	Belle	0.6, 1.4	[30]
ℓ_1	Belle	1, 1.4	[30]
ℓ_2	Belle	0.6, 1.4	[30]
ℓ_3	Belle	0.8, 1.2	[30]
h_1	Belle	0.7, 1.1, 1.3, 1.5	[31]
h_2	Belle	0.7, 0.9, 1.3	[31]
$h_{1,2}$	CDF	0.7	[32]
$h_{1,2}$	CLEO	1, 1.5	[33]
$\ell_{1,2,3}$	DELPHI	0	[34]
$h_{1,2,3}$	DELPHI	0	[34]

III. THEORETICAL ERRORS AND THEIR CORRELATIONS

The OPE description of semileptonic moments is subject to two sources of theoretical uncertainty: missing higher-order terms in Eq. (5) and terms that violate quark-hadron duality, namely, terms that are intrinsically beyond the OPE. We will attempt an estimate only of the first kind of uncertainty. The violation of local quark-hadron duality is expected to be suppressed in semileptonic B decays; it would manifest itself as an inconsistency of the fit, which as we will see is certainly not present at the current level of theoretical and experimental accuracy.

To estimate the effects due to higher-order corrections, we follow the method outlined in Ref. [21] and update it with the suggestions given in Ref. [20]: we assume that perturbative corrections can affect the Wilson coefficients of μ_π^2 and μ_G^2 at the level of $\pm 20\%$, while perturbative corrections and higher-power corrections can effectively change the coefficients of ρ_D^3 and $\rho_{\rm LS}^3$ by $\pm 30\%$. Moreover, we assign an irreducible theoretical uncertainty of 10 MeV to the heavy quark masses and vary $\alpha_s(m_b)$ by 0.02. The changes in M_i due to these variations of the fundamental parameters are added in quadrature and provide a theoretical uncertainty[1] $\delta M_i^{\rm th}$, to be subsequently added in quadrature with the experimental one, $\delta M_i^{\rm exp}$. This method is consistent with the residual scale dependence observed at NNLO and appears to be reliable: the NNLO corrections and the $O(1/m_b^{4,5})$ (using ground-state saturation as in Ref. [24]) have been found to be within the range of expectations based on the method in the original formulation of Ref. [21].

The correlation between theoretical errors assigned to different observables is much harder to estimate, but it plays an important role in the semileptonic fits, as will become clear in a moment. Let us first consider moments computed at a fixed value of $E_{\rm cut}$: as long as one deals with central higher moments, there is no argument of principle supporting a correlation between two different moments, for instance, ℓ_1 and h_2. We also do not observe any clear pattern in the known corrections and therefore regard the

[1]This theoretical uncertainty depends, of course, on the exact point in the parameter space. In practice, we adopt an iterative procedure recomputing the theory errors on the minimum χ^2 point till the process has converged.

theoretical predictions for different central moments as completely uncorrelated. When one computes the theory uncertainty with the method described above, one might think there are obvious correlations: suppose that both ℓ_1 and h_2 receive *positive* contributions from μ_π^2; by varying μ_π^2 by $\pm 20\%$, we see a positive correlation between ℓ_1 and h_2. But our aim was simply to have a rough estimate of the *size* of the theory uncertainty, and we make no claim to know the *exact magnitude* and *sign* of the higher-order correction. Therefore, the observed correlation is meaningless, and the safest assumption is to regard the theoretical predictions for different moments as uncorrelated.

Let us now consider the calculation of a certain moment M_i for two close values of $E_{\rm cut}$, say, 1 and 1.1 GeV. Clearly, the OPE expansion for $M_i(1\ \text{GeV})$ will be very similar to the one for $M_i(1.1\ \text{GeV})$, and we confidently expect this to be true at any order in α_s and $1/m_b$. The theoretical uncertainties we assign to $M_i(1\ \text{GeV})$ and $M_i(1.1\ \text{GeV})$ will therefore be very close to each other and *very highly correlated*. The degree of correlation between the theory uncertainty of $M_i(E_1)$ and $M_i(E_2)$ can intuitively be expected to decrease as $|E_1 - E_2|$ grows. Moreover, we know that higher-power corrections are going to modify significantly the spectrum only close to the endpoint. Indeed, one observes that the $O(1/m_b^{4,5})$ contributions are equal for all cuts below about 1.2 GeV (see Fig. 2 of Ref. [24]), and the same happens for the $O(\alpha_s\mu_\pi^2/m_b^2)$ corrections [22]. Therefore, the dominant sources of current theoretical uncertainty suggest very high correlations among the theoretical predictions of the moments for cuts below roughly 1.2 GeV.

In Refs. [7,9], it was assumed that the theoretical errors of moments at different values of $E_{\rm cut}$ are 100% correlated. This is too strong an assumption, which ends up distorting the fit, because the dependence of M_i on $E_{\rm cut}$, itself a function of the fit parameters, is then free of theoretical uncertainty. As a result, the uncertainty on the OPE parameters is underestimated. On the other hand, as we have just discussed, a high degree of correlation is to be expected if $E_{\rm cut}$ is not too large. Reference [8], which also presents a fit without theoretical errors, sets the theoretical correlation matrix equal to the experimental one. This probably underestimates correlations and would also imply no correlation between the theoretical prediction of the *same* observable measured by two independent experiments, which is unreasonable. Recent HFAG fits with the method of Ref. [8] do not present this problem.

An alternative approach consists in computing the correlation of the theoretical errors of $M_i(E_1)$ and $M_i(E_2)$ using the method we have used to estimate the theory uncertainty, namely, varying the values of the heavy quark expansion (HQE) parameters. This is, in fact, equivalent to assuming that the $E_{\rm cut}$ dependence of the unknown terms of the OPE follows closely the $E_{\rm cut}$ dependence of the known terms. It turns out that, in this way, the correlation is almost always very high.

Another possibility is to fix the correlation ξ between a moment M_i computed at $E_{\rm cut}$ and at $E_{\rm cut} + 0.1$ GeV, possibly with ξ higher for higher $E_{\rm cut}$. Following the reasoning above, ξ is naturally very close to 1 at low cuts and drops considerably at high cuts.

In our fits, we will consider the following four options:

(A) 100% correlation between moments at different cuts;
(B) correlations computed from theory predictions, as discussed above;
(C) constant scale factor $0 < \xi < 1$, with $\xi = 0.97$ for 100 MeV steps;
(D) a scale factor like in option C that depends on the cut, $\xi = \xi(E_{\rm cut})$, with

$$\xi(E_{\rm cut}) = 1 - \frac{1}{2} e^{-\frac{(E_0 - E_{\rm cut})}{\Delta}}, \tag{7}$$

where $E_0 \approx 1.75$ GeV is the partonic endpoint and Δ is an adjustable parameter, which we set at about 0.25 GeV.

As an illustration, the correlation between the theoretical errors of a generic moment with cuts at 0.6 and 1.2 GeV is 1 in scenario A; it depends on the specific moment, and it is generally quite close to 1 in scenario B; it is given by $\xi^6 = (0.97)^6 \simeq 0.83$ in scenario C; it is given by $\prod_{k=0}^{k=5} \xi(0.65 + 0.1k\ \text{GeV}) \simeq 0.88$ in scenario D. Similarly, the correlation between a moment measured at 1.3 and 1.5 GeV is approximately 0.94 in C and 0.76 in D.

In Fig. 1, we show the results of semileptonic fits performed with the four options for the theoretical correlations. The fits include all the data listed in Table I and the two constraints of Eq. (6). We add the experimental and theoretical covariance matrices, which is equivalent to adding the respective errors in quadrature.

In general, the results depend sensitively on the option adopted. In the case of the heavy quark masses, which are strongly correlated, we observe large errors that tend to increase in going from A to D, although the central values are quite consistent. The results of the fits for the nonperturbative parameters depend even stronger on the option; in particular, this is the case for μ_G^2, which has a very low value—incompatible with Eq. (6)—in scenario A and increases as correlations are relaxed.

Figure 1 also shows that the final uncertainty on some of the parameters can be much smaller than the "safety" range we have used in the evaluation of the theory errors. Consider, for instance, the final error on ρ_D^3: in scenario A, it is as low as 0.02, which is approximately 15% of the central value, much below the 30% we have employed. Evidently, the fit has found a direction in the parameter space with much lower uncertainty. On the other hand, when we relax the degree of correlation, as in options C and D, the final relative uncertainty on ρ_D^3 is close to 30%. In the next section, we will study the impact of additional constraints on the heavy quark masses on these fits.

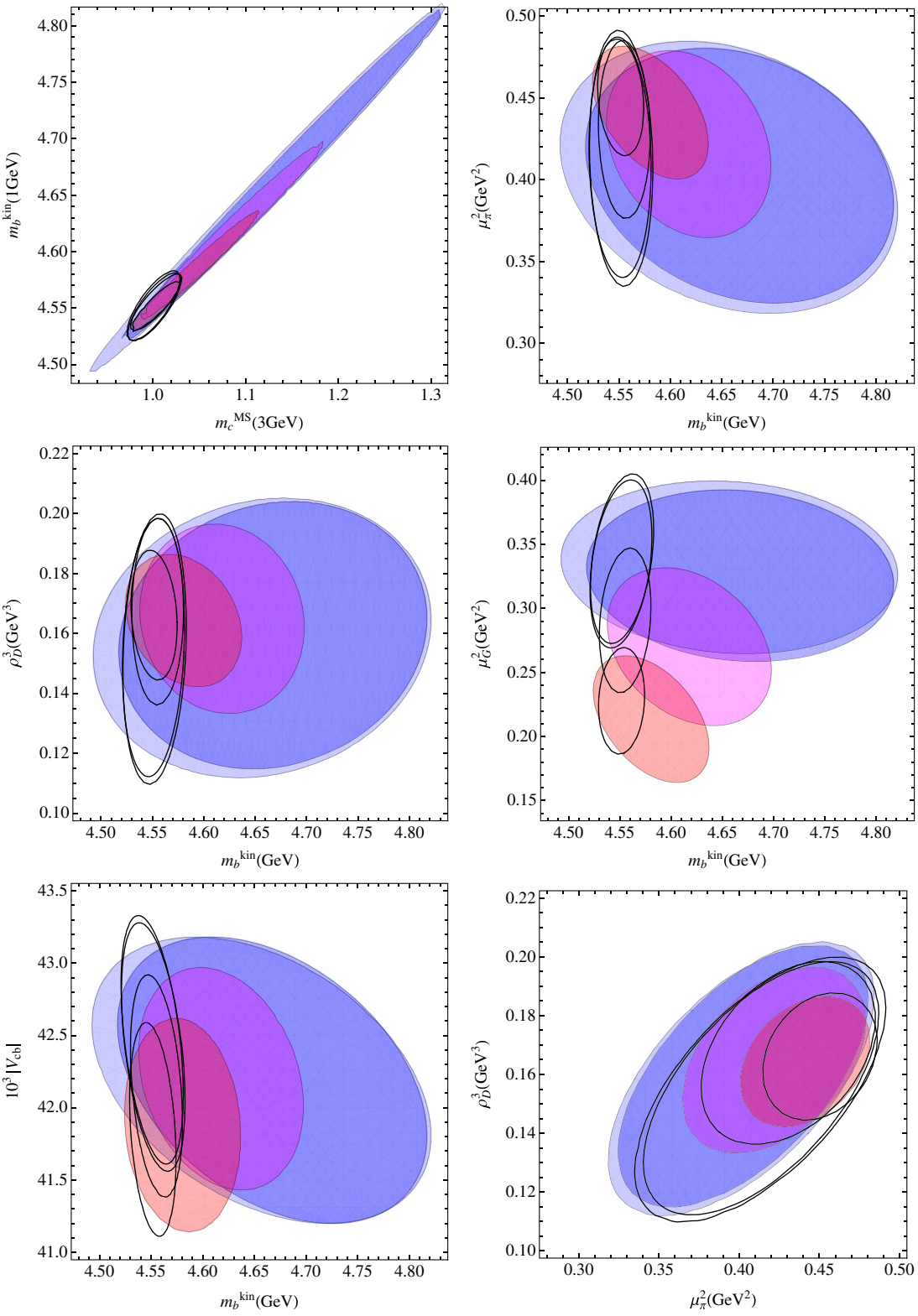

FIG. 1 (color online). Two-dimensional projections of the fits performed with different assumptions for the theoretical correlations. The orange, magenta, blue, and light blue 1-sigma regions correspond to scenarios A, B, C, D ($\Delta = 0.25$ GeV), respectively. The black contours show the same regions when the m_c constraint of Ref. [13] is employed.

IV. HEAVY QUARK MASS CONSTRAINTS

The inclusion of external precise constraints in the fit decreases the errors and may neutralize the ambiguity due to the ansatz for the theoretical correlations. It also allows us to check the consistency of the results with independent information. As semileptonic B decays alone determine precisely a linear combination of the heavy quark masses, approximately given by $m_b - 0.8m_c$, see the first plot in Fig. 1, a way to maximally exploit their potential consists of including in the fit one of the recent precise m_c determinations. A review of heavy quark mass determinations is beyond the scope of this paper; see, e.g., Refs. [3,35]. We simply list some of the most recent ones, for the charm mass,

(1) $\bar{m}_c(3\ \text{GeV}) = 0.986(13)\ \text{GeV}$ [11],
(2) $\bar{m}_c(3\ \text{GeV}) = 0.986(6)\ \text{GeV}$ [12],
(3) $\bar{m}_c(3\ \text{GeV}) = 0.994(26)\ \text{GeV}$ [13],

and for the bottom mass,

(1) $\bar{m}_b(\bar{m}_b) = 4.163(16)\ \text{GeV}$ [11],
(2) $\bar{m}_b(\bar{m}_b) = 4.164(23)\ \text{GeV}$ [12],
(3) $\bar{m}_b(\bar{m}_b) = 4.235(55)\ \text{GeV}$ [14],
(4) $\bar{m}_b(\bar{m}_b) = 4.247(34)\ \text{GeV}$ [15].

Here, all the masses are expressed in the $\overline{\text{MS}}$ scheme, and a relatively high scale, 3 GeV, is employed for the charm mass. In absolute terms, the charm mass is currently better determined than the bottom mass. This suggests computing the moments directly in terms of $\bar{m}_c(\bar{\mu})$, with $2 \lesssim \bar{\mu} \lesssim 3$ GeV, instead of using the charm mass in the kinetic scheme. The range of $\bar{\mu}$ is chosen to avoid large logarithms in our $O(\alpha_s^2)$ calculation and to minimize higher orders related to the definition of m_c, which necessarily involve $\alpha_s(\bar{\mu})$. This $\overline{\text{MS}}$ option for m_c is available in the code of Ref. [20] and avoids additional theoretical uncertainty due to the mass scheme conversion. In the case of the bottom mass, on the contrary, the common choice $\bar{m}_b(\bar{m}_b)$ is not well suited to the description of semileptonic B decays. In other words, the calculation of the moments in terms of $\bar{m}_b(\bar{m}_b)$ would lead to large higher-order corrections. While our predictions are always expressed in terms of the kinetic mass $m_b^{\text{kin}}(1\ \text{GeV})$, the above m_b constraints can be included after converting them to the kinetic scheme. Since the relation between the kinetic and the $\overline{\text{MS}}$ masses is known only to $O(\alpha_s^2)$, the ensuing uncertainty is not negligible. In Ref. [20], it was estimated to be about 30 MeV:

$$m_b^{\text{kin}}(1\ \text{GeV}) - \bar{m}_b(\bar{m}_b) = 0.37 \pm 0.03\ \text{GeV}. \quad (8)$$

The effect of the inclusion of charm mass constraints in the semileptonic fit is illustrated in Fig. 1, in which the determination of Ref. [13] is employed. As expected, the uncertainty in the b mass becomes smaller than 30 MeV in all scenarios, a marked improvement, also with respect to the precision resulting from the use of radiative moments [4]. On the other hand, there is hardly any improvement in the final precision of the nonperturbative parameters (see, for instance, the last plot, in the $\mu_\pi^2 - \rho_D^3$ plane).

TABLE II. b mass resulting from different m_c determinations. All masses are expressed in GeV.

$\bar{m}_c(3\ \text{GeV})$	$m_b^{\text{kin}}(1\ \text{GeV})$	$\bar{m}_b(\bar{m}_b)$
0.986(13) [11]	4.541(23)	4.171(38)
0.986(6) [12]	4.540(20)	4.170(36)
0.994(26) [13]	4.549(29)	4.179(42)

As already noted, the semileptonic moments are highly sensitive to a linear combination of the heavy quark masses. The constraints on m_b that we obtain using different m_c determinations in the fit are shown in Table II, where we have only considered option D with $\Delta = 0.25$ GeV. It is interesting to compare the results in the last column with the $\bar{m}_b(\bar{m}_b)$ determinations we have listed above. The bottom mass obtained using m_c given by the Karlsruhe group [11] is perfectly consistent with their own m_b result but also compatible with those of Refs. [12,14]. In general, lower values of m_b are preferred. The results depend little on the scenario chosen for the theory correlations: if we choose $\Delta = 0.2$ GeV, m_b gets lowered by 1 MeV in the first two rows and by 2 MeV in the third. Very similar results are found using alternative scenarios for the theory correlations. Of course, one can also include in the fit both m_c and m_b determinations, but because of the scheme translation error in m_b, the gain in accuracy will be limited.

When no external constraint is imposed on $m_{c,b}$, the semileptonic moments determine best a linear combination of the heavy quark masses that is very close to their difference. Using scenario D with $\Delta = 0.25$ GeV, we obtain

$$m_b^{\text{kin}}(1\ \text{GeV}) - 0.85\bar{m}_c(3\ \text{GeV}) = 3.701 \pm 0.019\ \text{GeV} \quad (9)$$

and similar results with the other scenarios (the error is as low as 12 MeV in scenario A). The ratio of the two masses is $\bar{m}_c(3\ \text{GeV})/m_b^{\text{kin}}(1\ \text{GeV}) = 0.2172(25)$. In the case the kinetic scheme is also adopted for m_c, the linear combination is slightly different, and Eq. (9) becomes

$$m_b^{\text{kin}}(1\ \text{GeV}) - 0.7m_c^{\text{kin}}(1\ \text{GeV}) = 3.784 \pm 0.019\ \text{GeV}. \quad (10)$$

The results of a few fits are reported in Table III–V. We choose the first one as our *default* fit. All the fits include a constraint on m_c, from either Ref. [11] or [13], and two fit both mass constraints from Ref. [11]. In the latter case, we have used Eq. (8) to translate

TABLE III. Global fits with m_c constraints. Scenario D has $\Delta = 0.25$ GeV. All parameters except m_c are in the kinetic scheme with cutoff at 1 GeV. The definition of m_c and the use of an m_b constraint are marked in the first column, directly under the reference for their constraints.

scenario	$m_b^{\rm kin}$	m_c	μ_π^2	ρ_D^3	μ_G^2	$\rho_{\rm LS}^3$	BR$_{c\ell\nu}$ (%)	$10^3\lvert V_{cb}\rvert$
D [11] $\bar m_c(3\ {\rm GeV})$	4.541	0.987	0.414	0.154	0.340	−0.147	10.65	42.42
	0.023	0.013	0.078	0.045	0.066	0.098	0.16	0.86
A [11] $\bar m_c(3\ {\rm GeV})$	4.540	0.987	0.454	0.167	0.234	−0.078	10.45	41.85
	0.014	0.013	0.035	0.022	0.040	0.085	0.13	0.74
B [11] $\bar m_c(3\ {\rm GeV})$	4.542	0.987	0.457	0.184	0.290	−0.135	10.51	42.15
	0.017	0.013	0.056	0.035	0.056	0.095	0.14	0.77
C [11] $\bar m_c(3\ {\rm GeV})$	4.539	0.987	0.415	0.155	0.336	−0.147	10.65	42.45
	0.022	0.013	0.073	0.043	0.066	0.098	0.16	0.86
D [11] $\bar m_c(3\ {\rm GeV})$, m_b	4.538	0.986	0.415	0.153	0.336	−0.145	10.65	42.46
	0.018	0.012	0.078	0.045	0.064	0.098	0.16	0.84
D [13] $\bar m_c(3\ {\rm GeV})$	4.549	0.996	0.413	0.154	0.339	−0.146	10.65	42.40
	0.029	0.026	0.078	0.045	0.066	0.098	0.16	0.87
D [11] $m_c^{\rm kin}$	4.548	1.092	0.428	0.158	0.344	−0.146	10.66	42.24
	0.023	0.020	0.079	0.045	0.066	0.098	0.16	0.85
D [11] $\bar m_c(2\ {\rm GeV})$, m_b	4.553	1.088	0.428	0.155	0.328	−0.139	10.67	42.42
	0.018	0.013	0.079	0.045	0.064	0.098	0.16	0.83

$\bar m_b(\bar m_b) = 4.163(16)$ GeV into $m_b^{\rm kin} = 4.533(32)$ GeV [the α_s dependence of Eq. (8) partly compensates that of $\bar m_b(\bar m_b)$]. The fits are generally good, with χ^2/degrees of freedom ranging from 0.32 for the default fit to 0.95 for case B and 1.18 for case A. The value of $\lvert V_{cb}\rvert$ is computed using

$$\lvert V_{cb}\rvert = \sqrt{\frac{\lvert V_{cb}\rvert^2 {\rm BR}_{c\ell\nu}}{\tau_B \Gamma^{\rm OPE}_{B\to X_c\ell\nu}}}, \tag{11}$$

with $\tau_B = 1.582(7)$ ps. Its theoretical error is computed combining in quadrature the parametric uncertainty that results from the fit and an additional 1.4% theoretical error to take into account missing higher-order corrections in the expression for the semileptonic width [20,36]. An approximate formula for $\lvert V_{cb}\rvert$ using the above τ_B value and $m_c(3\ {\rm GeV})$ is

$$\begin{aligned}\lvert V_{cb}\rvert = 0.042316[1 &+ 0.54(\alpha_s - 0.219) - 0.653(m_b^{\rm kin} - 4.55)\\ &+ 0.489(\bar m_c(3\,{\rm GeV}) - 1) + 0.016(\mu_\pi^2 - 0.44)\\ &+ 0.058(\mu_G^2 - 0.32) + 0.12(\rho_D^3 - 0.2)\\ &- 0.013(\rho_{\rm LS}^3 + 0.15)],\end{aligned} \tag{12}$$

where all dimensionful quantities are expressed in GeV.

A few comments are now in order:

(i) The inclusion of the m_c constraint has stabilized the fits with respect to the ansatz for the theory correlations. The only exception is represented by scenario A, which mostly deviates in the values of μ_π^2 and μ_G^2 and in the magnitude of the uncertainties. In any case, because of the above discussion, this scenario should be abandoned.

(ii) The low χ^2 of the default fit is due to the large theoretical uncertainties we have assumed. It may be tempting to interpret it as evidence that the theoretical

TABLE IV. Correlation matrix for the default fit: scenario D, $\Delta = 0.25$ GeV, m_c from Ref. [11].

$m_b^{\rm kin}$	$\bar m_c(3\,{\rm GeV})$	μ_π^2	ρ_D^3	μ_G^2	$\rho_{\rm LS}^3$	BR$_{c\ell\nu}$	$\lvert V_{cb}\rvert$
1	0.476	−0.101	0.218	0.484	−0.158	−0.092	−0.443
	1	−0.013	0.009	−0.014	0.004	0.012	−0.014
		1	0.613	0.007	0.056	0.126	0.342
			1	−0.041	−0.126	0.048	0.179
				1	−0.013	−0.023	−0.164
					1	−0.007	0.009
						1	0.461
							1

TABLE V. Correlation matrix for the fit with both m_c and m_b from Ref. [11], scenario D, $\Delta = 0.25$ GeV.

$m_b^{\rm kin}$	$\bar m_c(3\ {\rm GeV})$	μ_π^2	ρ_D^3	μ_G^2	$\rho_{\rm LS}^3$	BR$_{c\ell\nu}$	$\lvert V_{cb}\rvert$
1	0.405	−0.082	0.180	0.412	−0.130	−0.075	−0.389
	1	0.003	−0.027	−0.098	0.030	0.028	0.041
		1	0.626	0.025	0.051	0.123	0.338
			1	−0.080	−0.116	0.055	0.207
				1	0.013	−0.008	−0.120
					1	−0.012	−0.007
						1	0.463
							1

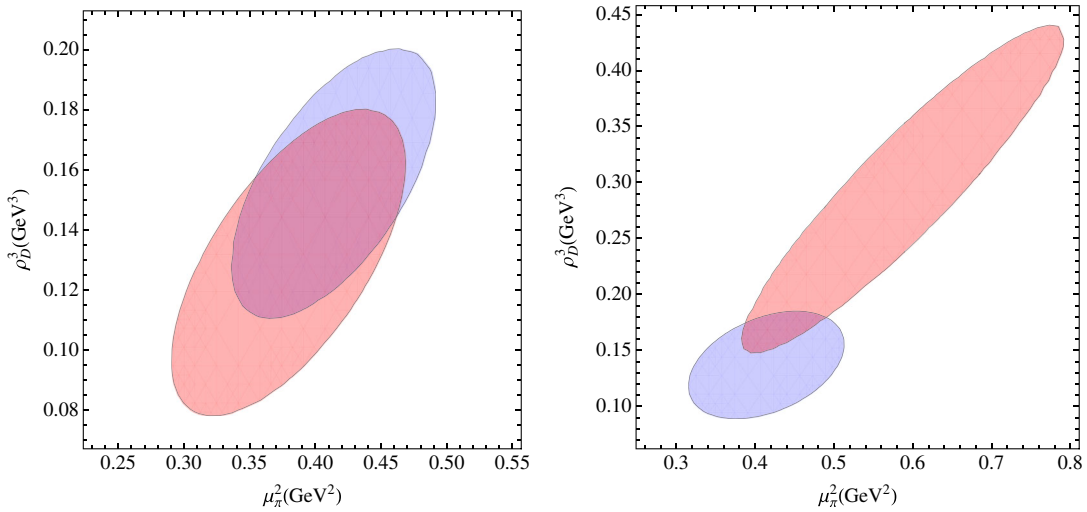

FIG. 2 (color online). 1σ projections on the $\mu_\pi^2 - \rho_D^3$ plane of the default fit. Left: with (blue) and without (red) moments measured at $E_{\mathrm{cut}} > 1.2$ GeV; right: with only hadronic moments (blue) and only leptonic moments (red).

errors have been overestimated. However, higher-order corrections may effectively shift the parameters of the $O(1/m_b^2)$ and $O(1/m_b^3)$ contributions. If we want to maintain the formal definition of these parameters, and to be able to use them elsewhere, we therefore have to take into account the potential shift they may experience because of higher-order effects.

(iii) The third hadronic moment by Delphi was neglected in previous analyses in the kinetic scheme. Its main effect on our default fit is to decrease ρ_D^3 by about 10% and μ_π^2 by about 3%.

(iv) The fits with a constraint on m_c are quite stable with respect to a change of inputs. In particular, we have found small differences when experimental data at high E_{cut} are excluded and when only hadronic or leptonic moments are considered. While the results for the heavy quark masses do not change appreciably, the results for the OPE parameters change within errors. We show in Fig. 2 the projection onto the $\mu_\pi^2 - \rho_D^3$ plane of the default fit with/without moments at $E_{\mathrm{cut}} > 1.2$ GeV and with only leptonic and only hadronic moments.

(v) One may wonder whether the inclusion of moments measured at different values of E_{cut} really benefits the final accuracy. We have run our default fit with only one E_{cut} for each moment per experiment and found slightly larger errors (26 MeV on m_b and 0.1 GeV^2 on μ_π^2) than when we use the full set of data. The benefit is therefore minor but not negligible. Of course, the inclusion of moments at different cuts plays a much more important role in scenarios A and B.

(vi) In the kinetic scheme, the inequalities $\mu_\pi^2(\mu) \geq \mu_G^2(\mu)$, $\rho_D^3(\mu) \geq -\rho_{\mathrm{LS}}^3(\mu)$ hold at arbitrary values of the cutoff μ. The central values of the fits always satisfy the inequalities.

(vii) The value of $|V_{cb}|$ is generally larger than in previous analyses. This is mostly due to the higher $\mathrm{BR}_{c\ell\nu}$, as can be seen in Table III. Indeed, the low value of $\mathrm{BR}_{c\ell\nu}$ is the most distinctive feature of scenarios A and B and the most relevant for the $|V_{cb}|$ determination. It is worth noting that the latest CKM global fit [1] gives $|V_{cb}| = 0.04273(77)$, with a marked preference for a high value of $|V_{cb}|$.

(viii) The $O(\alpha_s^2)$ perturbative expansion for the $b \to c\ell\nu$ width has relatively large coefficients when $\bar{m}_c(3\ \mathrm{GeV})$ is employed, while the situation improves in case one uses $\bar{m}_c(2\ \mathrm{GeV})$ or $m_c^{\mathrm{kin}}(1\ \mathrm{GeV})$; see the appendix of Ref. [20]. We have briefly studied what happens with $\bar{m}_c(2\ \mathrm{GeV})$: the answer depends little on the way one computes it from $\bar{m}_c(3\ \mathrm{GeV}) = 0.986(13)$ GeV. Using three-loop renormalization-group evolution leads to $\bar{m}_c(2\ \mathrm{GeV}) = 1.091(14)$ GeV, and in scenario D, one gets the results in the last row of Table III, with $|V_{cb}|$ very close to the other fits. Table III also reports results for a fit to the charm mass expressed in the kinetic scheme. In this case, we employ scenario D as in the default fit and use a constraint on $m_c^{\mathrm{kin}}(1\ \mathrm{GeV})$ derived from the $\bar{m}_c(3\ \mathrm{GeV})$ determination of Ref. [11]. Using the translation formula given in Ref. [20], we obtain $m_c^{\mathrm{kin}}(1\ \mathrm{GeV}) = 1.091 \pm 0.020$ GeV. The value of the $\mathrm{BR}_{c\ell\nu}$ and of $|V_{cb}|$ are consistent with the results of the $\overline{\mathrm{MS}}$ scheme fits.

Because of strong correlations, the measurements listed in Table I are only a subset of all the measured moments. To gain a visual appreciation of the quality of the default fit and to see how well it agrees also with the measurements that are not included, we show in Figs. 3 and 4 the leptonic and hadronic moments measurements compared with their theoretical prediction with theory uncertainty.

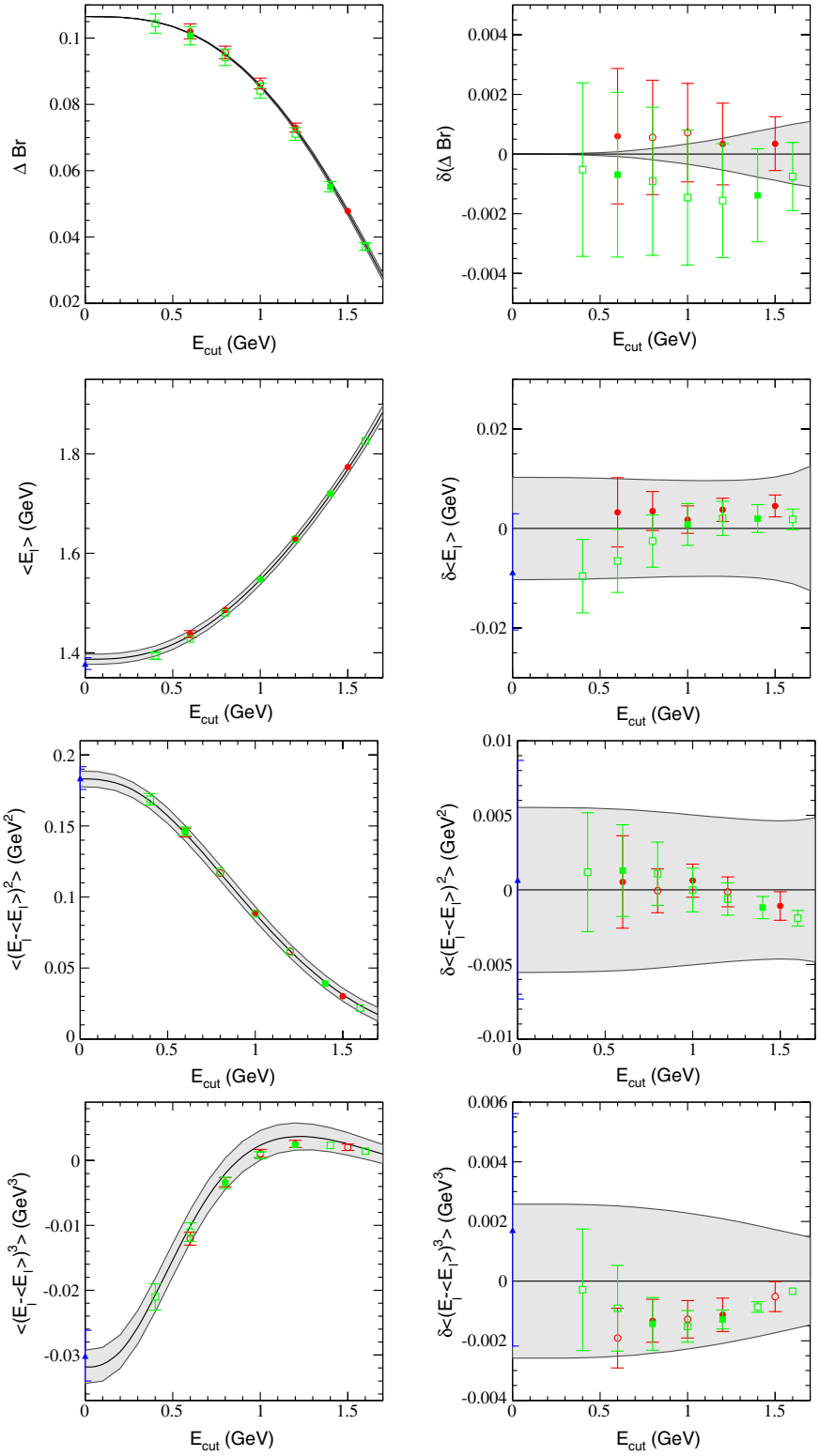

FIG. 3 (color online). Default fit predictions for R^*, $\ell_{1,2,3}$ compared with measured values in absolute terms (left) and as deviations (δ, right) from the predictions as a function of $E_{\rm cut}$. In all plots, the grey band is the theory prediction with total theory error. *BABAR* data are shown by circles, Belle by squares, and other experiments (DELPHI, CDF, and CLEO) by triangles. Filled symbols mean that the point was used in the fit. Open symbols are measurements that were not used in the fit.

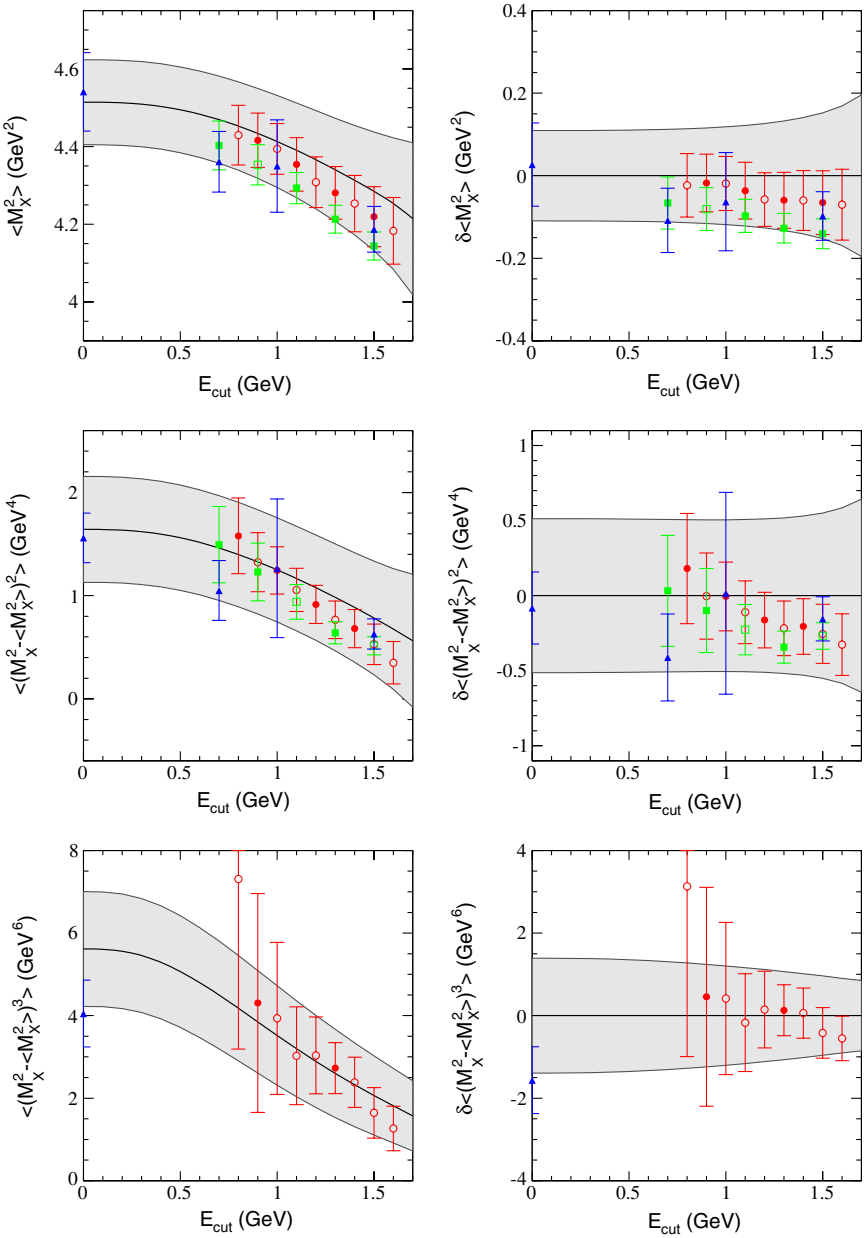

FIG. 4 (color online). Same as in Fig. 3 for $h_{1,2,3}$.

V. IMPLICATIONS OF THE DEFAULT FIT

A. Semileptonic phase space ratio

It is particularly convenient to normalize the branching fraction of the rare decays $B \to X_s\gamma$ and $B \to X_s\ell^+\ell^-$ to the semileptonic one, $\mathrm{BR}_{c\ell\nu}$. In this context, the semileptonic phase space ratio

$$C = \left|\frac{V_{ub}}{V_{cb}}\right|^2 \frac{\Gamma[\bar{B} \to X_c e\bar{\nu}]}{\Gamma[\bar{B} \to X_u e\bar{\nu}]} \tag{13}$$

is usually factorized [37–40]. C can be calculated using the OPE and the results of the fit to the semileptonic moments. In principle, the $B \to X_u\ell\bar{\nu}$ width is also sensitive to weak annihilation (WA) contributions, see, e.g., Ref. [40], which are poorly known but cancel out in the rare decay width. As far as the normalization of rare decays is concerned, WA effects can therefore be ignored. Even neglecting WA, however, the value of C does depend on the scale at which the WA matrix element is assumed to vanish. In the following, we follow Ref. [40] and use $\mu_{\mathrm{WA}} = m_b/2$.

In Ref. [40], C was computed in the kinetic scheme, based on the fits performed by HFAG at that time. The result was $C = 0.546 \pm 0.016(\mathrm{pert}) \pm 0.017(\mathrm{HQE})$, where the first uncertainty refers to higher-order perturbative contributions and the second is associated with the

semileptonic fit. A different result, $C = 0.582 \pm 0.016$, was reported in Ref. [8] in the 1S scheme; see also the first paper of Ref. [39] for additional details. The central value has already been converted to our convention with $\mu_{\rm WA} = m_b/2$. The discrepancy between these two values has now considerably reduced, as we will see in a moment.

To compute C with our default fit, we need to adapt the calculation of Ref. [40] to the use of a charm mass in the $\overline{\rm MS}$ scheme at $\mu = 2$ or 3 GeV. Here, we give the two corresponding approximate formulas,

$$\begin{aligned} C = g(\rho)\{&0.903 - 0.595\delta_{\alpha_s} + 0.0405\delta_b \\ &- 0.1137(\bar{m}_c(2\ \text{GeV}) - 1.05\ \text{GeV}) \\ &- 0.0184\mu_G^2 - 0.199\rho_D^3 + 0.004\rho_{\rm LS}^3\}, \end{aligned} \tag{14}$$

$$\begin{aligned} C = g(\rho)\{&0.849 - 0.92\delta_{\alpha_s} + 0.0596\delta_b \\ &- 0.2237(\bar{m}_c(3\ \text{GeV}) - 1\ \text{GeV}) - 0.0167\mu_G^2 \\ &- 0.203\rho_D^3 + 0.004\rho_{\rm LS}^3\}, \end{aligned} \tag{15}$$

where $g(\rho) = 1 - 8\rho + 8\rho^3 - \rho^4 - 12\rho^2 \ln\rho$, $\rho = (m_c/m_b)^2$, $\delta_{\alpha_s} = \alpha_s(4.6\ \text{GeV}) - 0.22$, and $\delta_b = m_b - 4.55$ GeV. The approximate formulas reproduce the complete calculation to better than 0.4% in the range $4.45 < m_b < 4.65$ GeV, $0.9 < \bar{m}_c(3\,\text{GeV}) < 1.1\,\text{GeV}$, $0.95 < \bar{m}_c(2\,\text{GeV}) < 1.15\,\text{GeV}$. Using our default fit, we obtain

$$C = 0.574 \pm 0.008, \tag{16}$$

with an additional ∼3% theoretical error. The result is identical if we include m_b from Ref. [11] in the fit. In scenario B with both $m_{c,b}$ from Ref. [11], we get $C = 0.572(8)$. In comparison with Ref. [40], the parametric uncertainty has reduced by a factor of 2, mostly thanks to the new charm mass constraint, and the central value has increased by about 1σ. Our result is in good agreement with that of Ref. [8].

One may worry that the perturbative series of C in terms of $\bar{m}_c(3\ \text{GeV})$ has relatively large coefficients, as witnessed by the strong α_s dependence in Eq. (15), and that it likely involves large $O(\alpha_s^3)$ terms. In this respect, the situation is somewhat better if one employs the kinetic charm mass or $\bar{m}_c(2\ \text{GeV})$; see Eq. (14). Evolving $\bar{m}_c(3\ \text{GeV}) = 0.986(13)$ GeV [11] down to 2 GeV, and using $\bar{m}_c(2\,\text{GeV}) = 1.091(14)$ GeV and $m_b^{\rm kin} = 4.533(32)$ GeV as constraints in a fit to $\bar{m}_c(2\ \text{GeV})$, we get

$$C = 0.566 \pm 0.008, \tag{17}$$

again with additional 3% theoretical uncertainty. This is compatible with the result in Eq. (16) and might be preferred as a reference value.

Let us now address the reasons behind the shift of C with respect to Ref. [40], due only to the different set of inputs. The fits we present in this paper, mostly because of the m_c constraint, have significantly lower m_b and m_c than those used in Ref. [40]. Figure 1 of Ref. [40] shows that by lowering the heavy quark masses one increases C and that heavy quark masses new central values lead to $C \approx 0.57$. It should also be stressed that in the absence of the m_c constraint option A for the theoretical correlations leads to higher m_b and m_c and to artificially smaller errors than B, C, and D [10]. Therefore, previous fits in the kinetic scheme preferred a lower C and underestimated its uncertainty. The analogous effect on $|V_{cb}|$ was negligible. This is also the main reason for the discrepancy between the values of C in Refs. [40] and [8]. There are other differences between these two analyses (experimental inputs, scheme, etc.), but this is the most important component.

Of course, the factor C is just one component of the calculation of rare B decays. What actually enters inclusive B decays is $\text{BR}_{c\ell\nu}/C$, and there are additional power-suppressed corrections that affect the width and depend on the same parameters that determine C, as well as charm loops in the perturbative corrections. As precision increases, it is no longer obvious that the factorization of C is still advantageous, except as a bookkeeping device. Nevertheless, the results of our fit, with the complete correlation matrix, are all one needs for a careful analysis of the parametric uncertainty in those cases.

Finally, it is worth reminding the reader that, in the case of $B \to X_s\gamma$, it is often necessary to extrapolate measurements performed with a cut on the photon energy higher than about 1.6 GeV to lower photon energies, at which the local OPE is expected to work better. This extrapolation can be performed using different techniques [41], but it crucially depends on precise HQE parameters, namely, on the results of semileptonic fits.

B. Local contributions to the zero-recoil sum rule

The $B \to D^*\ell\nu$ form factor at zero recoil can be estimated using heavy quark sum rules [6,42]. The form factor $\mathcal{F}(1)$ is obtained by separating the elastic $B \to D^*$ transition contribution from the total inelastic transition at zero recoil,

$$I_0(\varepsilon_M) = \mathcal{F}^2(1) + I_{\rm inel}(\varepsilon_M), \tag{18}$$

where $I_{\rm inel}(\varepsilon_M)$ is related to the sum of the differential decay probabilities into the excited states with mass up to $M_{D^*} + \varepsilon_M$ in the zero-recoil kinematics.

The OPE allows us to calculate the amplitude $I_0(\varepsilon_M)$ in the short-distance expansion, provided $|\varepsilon|$ is sufficiently large compared to the ordinary hadronic mass scale. Setting $\varepsilon = \mu^{\rm kin}$,

$$I_0(\mu^{\rm kin}) = \xi_A^{\rm pert}(\mu^{\rm kin}) - \Delta_{1/m^2} - \Delta_{1/m^3} + \cdots, \tag{19}$$

where the ellipses stand for higher-order contributions and $\xi_A^{\rm pert}$ represents a perturbative contribution. The latter was computed in Ref. [6] to $O(\alpha_s^2)$: $\sqrt{\xi_A^{\rm pert}}(0.75\ {\rm GeV}) = 0.98 \pm 0.01$. The leading power contributions to I_0 were calculated in Refs. [42] to order $1/m_Q^2$ and in Ref. [43] to order $1/m_Q^3$ and read

$$\Delta_{1/m^2} = \frac{\mu_G^2}{3m_c^2} + \frac{\mu_\pi^2 - \mu_G^2}{4}\left(\frac{1}{m_c^2} + \frac{2}{3m_c m_b} + \frac{1}{m_b^2}\right),$$
$$\Delta_{1/m^3} = \frac{\rho_D^3 - \frac{1}{3}\rho_{\rm LS}^3}{4m_c^3} + \frac{1}{12m_b}\left(\frac{1}{m_c^2} + \frac{1}{m_c m_b} + \frac{3}{m_b^2}\right)(\rho_D^3 + \rho_{\rm LS}^3).$$

In the kinetic scheme, the nonperturbative parameters μ_π^2, μ_G^2, ρ_D^3, and $\rho_{\rm LS}^3$ all depend on the hard Wilsonian cutoff $\mu^{\rm kin}$. Since the heavy quark expansion of I_0 involves inverse powers of m_c, the cutoff must satisfy $\mu^{\rm kin} \ll 2m_c$, and it is better to have it lower than 1 GeV. We therefore take the values of the OPE parameters extracted from our default fit with m_c in the kinetic scheme, evolve them down to $\mu^{\rm kin} = 0.75$ GeV, and find

$$\Delta_{1/m^2} = 0.084 \pm 0.017, \qquad \Delta_{1/m^3} = 0.021 \pm 0.008, \tag{20}$$

and for the sum,

$$\Delta_{1/m^2} + \Delta_{1/m^3} = 0.104 \pm 0.023. \tag{21}$$

If we use scenario B, we get a slightly larger value 0.111 ± 0.016, closer to the preliminary result 0.118 ± 0.015 given in Ref. [6] and obtained using that scenario. The quantity in Eq. (21) is an important ingredient of the heavy quark sum rule estimate of $\mathcal{F}(1)$; the present update does not affect significantly the results of Ref. [6].

C. Impact on inclusive $|V_{ub}|$ determination

To get a rough estimate of the precision that can be reached applying the results of our default fit to the semileptonic $B \to X_u \ell\nu$ analyses, we use the information given in the kinetic scheme analysis of Ref. [44]. Recent experimental studies have considered lower cutoffs on the lepton momentum as low as 1 GeV, which is very close to the total decay width and for which a local OPE description is perfectly adequate. Therefore, we take Eq. (45) of Ref. [44] and compute the parametric uncertainty on the total $B \to X_u \ell\nu$ width using the results of the default fit. We obtain a 2.2% error that translates into a 1.1% parametric uncertainty on $|V_{ub}|$. A slightly smaller uncertainty, 1.8%, is obtained if one employs a fit that also includes the constraint on m_b from Ref. [11]. Since the uncertainty is dominated by that of m_b, better determinations of this mass will result in further reduction of the parametric error.

In summary, the parametric uncertainty on the total $B \to X_u \ell\nu$ width is about 2% and can be reduced in the future; it will have to be considered together with a $\gtrsim 1\%$ theoretical uncertainty. As mentioned above, this should essentially hold even when a lower cut on the lepton momentum around 1 GeV is applied. On the other hand, for higher cuts, the local OPE is no longer sufficient, and the sensitivity to m_b gets stronger; these analyses will benefit from a better determination of m_b even more.

VI. SUMMARY

In this paper, we have reassessed the whole strategy of global fits to the semileptonic moments. We have shown that the results depend sensitively not only on the estimate of the theoretical uncertainties but also on the assumptions about their correlation. We have studied the impact of precise determinations of the heavy quark masses from independent data on the global fits and shown that their use leads to more precise results, which depend less on the assumptions on the theoretical correlations. Using a determination of m_c with 13 MeV uncertainty, we were able to determine m_b within about 20 MeV, in good agreement and competitive with some of the most precise m_b determinations. In the absence of external constraints on the heavy quark masses, the semileptonic moments determine their difference with a 20 MeV uncertainty; see Eq. (9). This is a robust NNLO relation that we find stable against theoretical assumptions.

The value of $|V_{cb}|$ that we obtain is higher than in previous analyses but compatible with the prediction of a global CKM fit in the Standard Model [1]; it has a total 2% accuracy, which is dominated by theoretical errors. We have also studied the impact of the new fits on the calculation of the semileptonic phase space ratio C, on the power corrections to the zero-recoil sum rule, and on the extraction of $|V_{ub}|$.

Theoretical uncertainties are the major obstacle to an accurate determination of $|V_{cb}|$ using inclusive semileptonic B decays. Our theoretical errors are essentially determined by a conservative estimate of the dominant sources of higher-order corrections. There are therefore good prospects for improvement, related to the completion of the calculation of $O(\alpha_s \mu_G^2/m_b^2)$ and to the inclusion of the $O(1/m_Q^{4,5})$ corrections. A more significant reduction of the error on $|V_{cb}|$ will also require a calculation of perturbative corrections to the coefficient of the Darwin operator. In contrast, the experimental situation is much better at the moment and will further improve at Belle II.

ACKNOWLEDGMENTS

P. G. is grateful to Lorenzo Magnea and to the late Kolya Uraltsev for useful discussions and to Mikolaj Misiak and Matthias Steinhauser for carefully reading a preliminary version of this paper. This work is supported in part by MIUR under Contract No. 2010YJ2NYW_006.

[1] M. Bona *et al.* (UTFit Collaboration), J. High Energy Phys. 10 (**2006**) 081; http://utfit.org for the Winter 2013 update; see also CKMfitter Collaboration, http://ckmfitter.in2p3.fr.

[2] I. I. Bigi, N. G. Uraltsev, and A. Vainshtein, Phys. Lett. B **293**, 430 (1992); I. I. Bigi, M. Shifman, N. G. Uraltsev, and A. Vainshtein, Phys. Rev. Lett. **71**, 496 (1993); B. Blok, L. Koyrakh, M. Shifman, and A. I. Vainshtein, Phys. Rev. D **49**, 3356 (1994); A. V. Manohar and M. B. Wise, *ibid.* **49**, 1310 (1994).

[3] M. Antonelli *et al.*, Phys. Rep. **494**, 197 (2010).

[4] Y. Amhis *et al.* (Heavy Flavor Averaging Group [HFAG]), arXiv:1207.1158.

[5] J. A. Bailey *et al.* (Fermilab Lattice and MILC Collaborations), Proc. Sci., LATTIC (**2010**), 311.

[6] P. Gambino, T. Mannel, and N. Uraltsev, J. High Energy Phys. 10 (**2012**) 169; Phys. Rev. D **81**, 113002 (2010).

[7] B. Aubert *et al.* (*BABAR* Collaboration.), Phys. Rev. Lett. **93**, 011803 (2004).

[8] C. W. Bauer, Z. Ligeti, M. Luke, A. V. Manohar, and M. Trott, Phys. Rev. D **70**, 094017 (2004).

[9] O. L. Buchmuller and H. U. Flacher, Phys. Rev. D **73**, 073008 (2006).

[10] P. Gambino and C. Schwanda, arXiv:1102.0210.

[11] K. G. Chetyrkin, J. H. Kuhn, A. Maier, P. Maierhofer, P. Marquard, M. Steinhauser, and C. Sturm, Phys. Rev. D **80**, 074010 (2009).

[12] I. Allison *et al.* (HPQCD Collaboration), Phys. Rev. D **78**, 054513 (2008); C. McNeile, C. T. H. Davies, E. Follana, K. Hornbostel, and G. P. Lepage (HPQCD Collaboration), *ibid.* **82**, 034512 (2010).

[13] B. Dehnadi, A. H. Hoang, V. Mateu, and S. M. Zebarjad, J. High Energy Phys. 09 (**2013**) 103.

[14] A. Hoang, P. Ruiz-Femenia, and M. Stahlhofen, J. High Energy Phys. 10 (**2012**) 188.

[15] W. Lucha, D. Melikhov, and S. Simula, Phys. Rev. D **88**, 056011 (2013).

[16] G. Paz, arXiv:1011.4953.

[17] A. Pak and A. Czarnecki, Phys. Rev. Lett. **100**, 241807 (2008).

[18] K. Melnikov, Phys. Lett. B **666**, 336 (2008).

[19] S. Biswas and K. Melnikov, J. High Energy Phys. 02 (**2010**) 089.

[20] P. Gambino, J. High Energy Phys. 09 (**2011**) 055.

[21] P. Gambino and N. Uraltsev, Eur. Phys. J. C **34**, 181 (2004).

[22] T. Becher, H. Boos, and E. Lunghi, J. High Energy Phys. 12 (**2007**) 062.

[23] A. Alberti, T. Ewerth, P. Gambino, and S. Nandi, Nucl. Phys. **B870**, 16 (2013).

[24] T. Mannel, S. Turczyk, and N. Uraltsev, J. High Energy Phys. 11 (**2010**) 109.

[25] M. Gremm and A. Kapustin, Phys. Rev. D **55**, 6924 (1997).

[26] I. I. Y. Bigi, M. A. Shifman, N. Uraltsev, and A. I. Vainshtein, Phys. Rev. D **56**, 4017 (1997); Phys. Rev. D**52**, 196 (1995).

[27] N. Uraltsev, Phys. Lett. B **545**, 337 (2002).

[28] B. Aubert *et al.* (*BABAR* Collaboration), Phys. Rev. D **81**, 032003 (2010).

[29] B. Aubert *et al.* (*BABAR* Collaboration), Phys. Rev. D **69**, 111104 (2004).

[30] P. Urquijo *et al.*, Phys. Rev. D **75**, 032001 (2007).

[31] C. Schwanda *et al.* (BELLE Collaboration), Phys. Rev. D **75**, 032005 (2007).

[32] D. E. Acosta *et al.* (CDF Collaboration), Phys. Rev. D **71**, 051103 (2005).

[33] S. E. Csorna *et al.* (CLEO Collaboration), Phys. Rev. D **70**, 032002 (2004).

[34] J. Abdallah *et al.* (DELPHI Collaboration), Eur. Phys. J. C **45**, 35 (2006).

[35] J. Beringer *et al.* (Particle Data Group), Phys. Rev. D **86**, 010001 (2012).

[36] D. Benson, I. I. Bigi, T. Mannel, and N. Uraltsev, Nucl. Phys. **B665**, 367 (2003).

[37] P. Gambino and M. Misiak, Nucl. Phys. **B611**, 338 (2001).

[38] C. Bobeth, P. Gambino, M. Gorbahn, and U. Haisch, J. High Energy Phys. 04 (**2004**) 071.

[39] M. Misiak and M. Steinhauser, Nucl. Phys. **B764**, 62 (2007); M. Misiak *et al.*, Phys. Rev. Lett. **98**, 022002 (2007).

[40] P. Gambino and P. Giordano, Phys. Lett. B **669**, 69 (2008).

[41] D. Benson, I. I. Bigi and N. Uraltsev, Nucl. Phys. **B710**. 371 (2005); M. Neubert, Eur. Phys. J. C **40**, 165 (2005).

[42] I. Bigi, M. Shifman, N. G. Uraltsev, and A. Vainshtein, Phys. Rev. D **52**, 196 (1995); M. A. Shifman, N. G. Uraltsev, and A. I. Vainshtein, *ibid.* **51**, 2217 (1995).

[43] I. Bigi, M Shifman, and N. G. Uraltsev, Annu. Rev. Nucl. Part. Sci. **47**, 591 (1997).

[44] P. Gambino, P. Giordano, G. Ossola, and N. Uraltsev, J. High Energy Phys. 10 (**2007**) 058.